



**HAL**  
open science

## 40 W of supercontinuum generated by a self-pulsed pump-sharing oscillator-amplifier

Clara Abbouab, Marie-Alicia Malleville, Baptiste Leconte, Raphaël Jamier, Etienne Genier, Philippe Morin, Philippe Roy

► **To cite this version:**

Clara Abbouab, Marie-Alicia Malleville, Baptiste Leconte, Raphaël Jamier, Etienne Genier, et al.. 40 W of supercontinuum generated by a self-pulsed pump-sharing oscillator-amplifier. *Applied optics*, 2024, 63 (2), pp.377-382. 10.1364/ao.511239 . hal-04372401

**HAL Id: hal-04372401**

**<https://hal.science/hal-04372401>**

Submitted on 4 Jan 2024

**HAL** is a multi-disciplinary open access archive for the deposit and dissemination of scientific research documents, whether they are published or not. The documents may come from teaching and research institutions in France or abroad, or from public or private research centers.

L'archive ouverte pluridisciplinaire **HAL**, est destinée au dépôt et à la diffusion de documents scientifiques de niveau recherche, publiés ou non, émanant des établissements d'enseignement et de recherche français ou étrangers, des laboratoires publics ou privés.

# 40 W OF SUPERCONTINUUM GENERATED BY A SELF-PULSED PUMP-SHARING OSCILLATOR-AMPLIFIER

CLARA ABBOUAB<sup>1,2,\*</sup>, MARIE-ALICIA MALLEVILLE<sup>1</sup>, BAPTISTE LECONTE<sup>1</sup>, RAPHAËL JAMIER<sup>1</sup>, ETIENNE GENIER<sup>2</sup>, PHILIPPE MORIN<sup>2</sup> AND PHILIPPE ROY<sup>1</sup>

<sup>1</sup> XLIM research Institute, University of Limoges, CNRS, UMR 7252, F-87000 Limoges, France

<sup>2</sup> CILAS, 8 avenue Buffon, CS16319, F-45063 Orleans cedex2, France

\*clara.abbouab@xlim.fr

Received 5 November 2023; revised 30 November 2023; accepted 30 November 2023; posted 1 December 2023; published 3 January 2024

**We demonstrate an all-fiber supercontinuum (SC) source delivering up to 40 W of average power ranging from 750 to 2200 nm. The laser source is based on a self-Q-switched pump-sharing oscillator-amplifier. The self-Q-switched master oscillator generates giant pulses, amplified in the high-power stage. Finally, a passive fiber acts as a nonlinear stage improving the spectrum flatness as well as the spectral broadening. To the best of our knowledge, this is the first time that a pump-sharing oscillator-amplifier is used for SC generation and based on the use of a submeter Ytterbium-doped fiber length inside the oscillator.**

© 2024 Optica Publishing Group

<https://doi.org/10.1364/AO.511239>

## 1. INTRODUCTION

High-power supercontinuum (SC) laser sources are currently of increased interest for remote environmental sensing and military applications [1–4]. Consequently, research activities aim to improve output power and the spectral broadening of the laser as well as its flatness [5,6]. In 2018, Zhao *et al.* reported an all-fiber supercontinuum source delivering an average power of 215 W with a spectrum spanning from 480 nm to beyond 2000 nm. This source was obtained by injecting amplified picosecond pulses into a piece of 5 m-long PCF with a 4.8  $\mu\text{m}$  core diameter [7]. Another SC source going from 390 to 2400 nm with 314.7 W average output power, was also achieved by pumping, with picosecond pulses having an average power of 942 W, a 14 m-long tapered PCF with a core diameter varying from 4.2  $\mu\text{m}$  to 3.3  $\mu\text{m}$ . The authors achieved a coupling efficiency of about 63.7% thanks to the development of a mode field adaptor between the amplifier stage and the PCF [8]. However, the power scaling in SC sources including a PCF is quite limited by the power handling capabilities of the very small core and the low coupling efficiency into the PCF and through the splice between the nonlinear fiber and the amplification chain. The latter point suffers a severe thermal load due to modal mismatch.

Otherwise, large mode area ytterbium-doped double-clad fibers (DC-LMA-YDFs), which are key components for multi-kW range laser sources operating in the continuous wave regime, also face nonlinear limits due to long interaction lengths between silica core and high guided power levels, despite core diameter larger than 20  $\mu\text{m}$  [9]. Using such fibers can overcome the issues mentioned above with PCFs, enabling a high coupling efficiency between the

amplifier stage and the non-linear stage of the laser source and offering the opportunity to handle very high average powers. Moreover, they can be used to amplify and broaden the initial seed spectrum. Some master oscillator power amplifier (MOPA) systems for high-power SC generation including multiple amplification chains are reported in the following literature.

For example, in 2023, Jiang *et al.* reported a 714 W SC source with a spectrum ranging from 690 nm to 2350 nm and a spectrum spanning from 1050 nm to 2095 nm (at -10 dB) [5]. The system includes both, a four-stage MOPA configuration for the power scaling starting from a 15 ns low-power seed laser at 1065 nm and a 20 m-long piece of passive 30/600  $\mu\text{m}$  (core/cladding diameters) fiber. The latter perfectly matches the opto-geometrical characteristics of the active fiber used in the last power amplification stage and is used to optimize the spectrum performances. Since the peak power of the incident laser is low, and the system consists of large MFD fiber pumped by a CW source, the only way to increase the nonlinearities and spread the spectrum is to increase the fiber length. In 2022, a 3 kW SC source spanning from 925 nm to 1862 nm (with a 20 dB bandwidth of 574 nm) was obtained using a configuration including a Raman fiber laser oscillator and a YDF laser oscillator as multi-wavelength seeds for the fiber amplifier of 40 m followed by a piece of 415 m germanium-doped fiber (GDF) [6]. Signals coming from the Raman fiber laser and the YDF laser, are then amplified through an active fiber with core/cladding diameters of 46/400  $\mu\text{m}$ . Finally, they propagate through the passive fiber, with the same core/cladding diameters as the active fiber, for the SC generation.

The two aforementioned configurations based on, at least, four stages for SC generation, are quite complex, expensive, cumbersome, and difficult to implement in portable systems. Recently, researchers worked on a structure called “oscillating-amplifying integrated fiber laser” (OAIFL) as a simpler method for power scaling compared to the classical MOPA structure [10]. Indeed, due to the lack of any isolator or cladding power stripper (CPS) between the seeder and the amplifier, the unabsorbed forward pump light emerging from the oscillator can pump the amplification stage. In the case of a bi-directional pumping scheme, the residual backward pump light can also enter the oscillating section. In 2021, an OAIFL system achieved a power of up to 3.5 kW at 1080 nm [10]. To do so, the fiber lengths integrated are about 8 meters in the seeder and around 18 meters in the amplifier stage when using ytterbium-doped fibers (YDF) with core/cladding diameters of 22/400  $\mu\text{m}$  and a cladding absorption coefficient at 976 nm of approximately 2.6 dB/m. In 2022, a particular OAIFL named “pump-sharing oscillator-amplifier” (PSOA) with a shorter active fiber length of 1.6 m was reported [11]. In this work, the laser delivered 3.1 kW of power at 1050 nm with an  $M^2$  of 1.33. However, the authors did not investigate the temporal dynamics resulting from the very high level of unabsorbed pump power in the oscillator. Furthermore, neither study has been led on SC generation through a PSOA.

In this paper, we propose a method for SC generation based on a pump-sharing oscillator-amplifier. The PSOA is designed to be as simple as possible. The seeder stage is temporally unstable and transmits almost all the pump power to the amplifier stage thanks to a very short intracavity active fiber length. Respectively both the power amplifier and the nonlinear frequency conversion stages are simply made of active and passive 20/400  $\mu\text{m}$  core/cladding diameters fibers. With this all-fiber PSOA SC source, we obtained up to 40.7 W of average power ranging from 750 nm to 2200 nm. To the best of our knowledge, this is the first time that a pump-sharing oscillator-amplifier is

used for SC generation and based on the use of a submeter YDF length inside the oscillator.

## 2. EXPERIMENTAL SET-UP

The experimental set-up developed here is a PSOA structure and consists of three stages which are a master oscillator with a short cavity length, a fiber amplifier, and a nonlinear frequency conversion stage as shown in Fig. 1. The nonlinear stage consists of a piece of passive fiber perfectly matching the opto-geometrical characteristics of the active fiber used for the seeder and amplifier stage. Concerning the first stage, the resonant cavity is made of a high reflectivity (99.8 %) fiber Bragg grating (HR-FBG) on one side and a low reflectivity (10.1 %) output coupler fiber Bragg grating (OC-FBG) on the other side with a spectral linewidth of 3 and 1.03 nm, respectively. Both gratings are commercially sourced, are centered at 1080 nm and are written on a 20/400  $\mu\text{m}$  passive fiber. A short piece of 0.8 m-long YDF with a core diameter of 20  $\mu\text{m}$  and an inner-cladding diameter of 400  $\mu\text{m}$  is used as the gain medium. Its peak cladding absorption is 1.7 dB/m at 976 nm and its zero-dispersion wavelength (ZDW) is near to 1.3  $\mu\text{m}$ . This YDF is curved on a diameter of 21 cm to filter the high-order transversal modes and only emits the fundamental mode. The YDF has been previously tested with this curvature in a free space cavity to ensure the singlemodeness of the output beam. Indeed, the measure of the  $M^2$  values gave 1.07 and 1.08 at a pump power of 50 W, and another measure with a supercontinuum source and a high pass filter with a cutting wavelength at 1075 nm, showed that only the fundamental mode could be excited. A single 140 W 976nm wavelength-locked fiber-coupled Laser Diode (LD) is used as a forward CW pump source.

The pump power is coupled into the active fiber cladding through a  $(6+1)\times 1$  multimode combiner located in the seeder cavity. Considering the very short cavity length as well as the cladding absorption coefficient at 976 nm of the YDF, the level of absorbed pump power will be very low in the

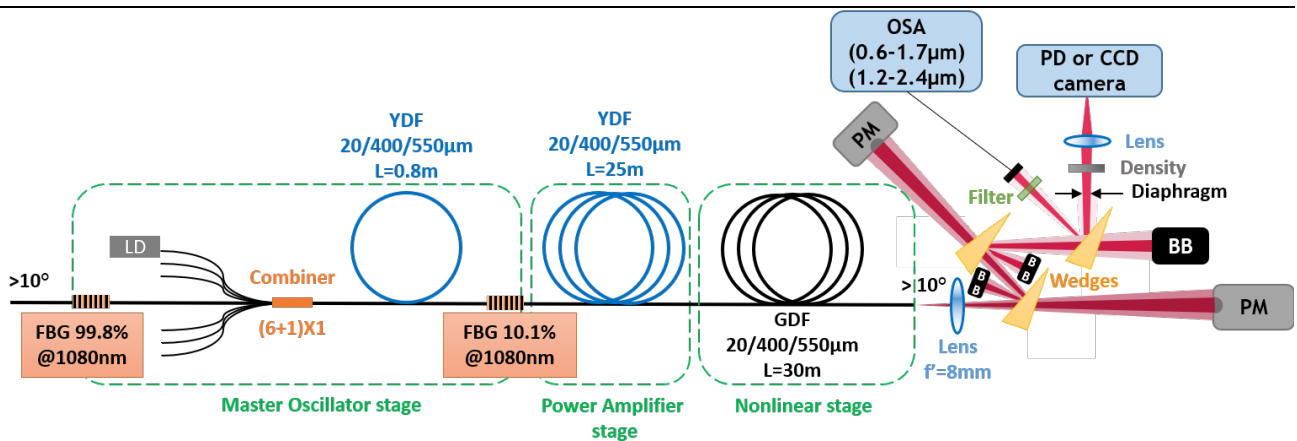


Fig. 1. Schematic of the PSOA experimental setup and optical bench measurement. BB = Beam Block, PM = Power Meter.

seeder stage meaning that the residual pump power at the end of the oscillator will be mainly absorbed in the power amplification stage. As a consequence of the very low level of absorbed pump power, the emitted signal is self-pulsed without any inner cavity amplitude modulator. This is a common signature of the passive Q-switching lasing method which generates pulses using a saturable absorber [12]. The pulses are then amplified thanks to the residual pump power entering into the second stage which is made of a 25 m-long section YDF with the same core/clad diameters and absorption as the doped fiber used in the master oscillator.

Finally, the third stage is composed of a 30 m-long piece of 20/400  $\mu\text{m}$  passive GDF which contributes to the spectral broadening. The free port of the HR-FBG and the final output fiber end were angle-cleaved to avoid any parasitic lasing effect coming from the resonant cavity due to the Fresnel reflection at the silica-air interfaces. The output signal power, the residual pump power, the spectra, and the temporal dynamics were monitored at the end of each stage. For this purpose, the output power in the core of the beam of the SC laser was measured with a wavelength-insensitive power meter. Indeed, the power meter was placed so that the core of the beam covered its full cell area while the cladding beam was blocked. Far-field intensity distributions, at the output of the GDF, were recorded with a commercial CCD camera. The spectra were collected at low power through a multimode fiber (MMF) and recorded thanks to two different optical spectrum analyzers (OSA) covering the short wavelengths (from 600 to 1700 nm) and long ones (from 1200 to 2400 nm). To reduce the influence of the multi-order diffraction during the measurement process, a long wavelength-pass filter with a cutoff wavelength of 1400 nm was used when recording the long-wavelength OSA. The final spectrum was made of the coupling of each OSA's spectrum by aligning their spectral intensity level. Finally, a photodiode (PD) and an oscilloscope having a 100 MHz bandwidth were employed for temporal dynamics characterizations.

### 3. EXPERIMENTAL RESULTS AND DISCUSSION

#### Experimental results at the output of the master oscillator stage

Fig. 2 shows the evolution of both the emitted signal power (red line) and the residual pump power (blue line) at the output of the seeder considered independently as a function of pump power. At a pump power of 143 W, we measure, at the oscillator's output, an average signal power of 11 W. Therefore, 92% of the pump power is transmitted to the amplification stage and thus only 8% of the pump power is absorbed in the short piece of YDF and generates signal power.

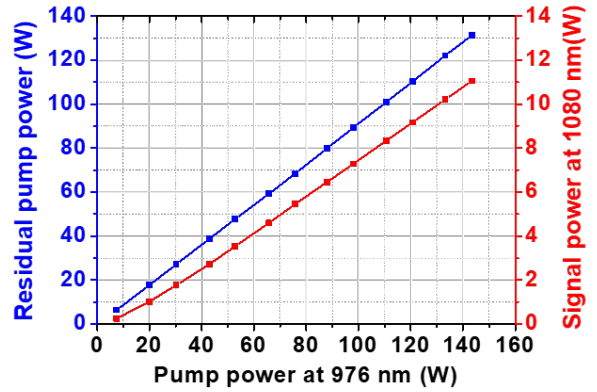


Fig. 2. Evolution of the signal (red curve) and residual power pump transmitted in the amplifier stage (blue curve) as a function of input pump power.

Fig. 3 shows the spectral evolution measured at the output of the seeder when increasing the pump power from 30 W up to 143 W. We observe the signal wavelength is 1080 nm without any significant spectral broadening when increasing the pump power.

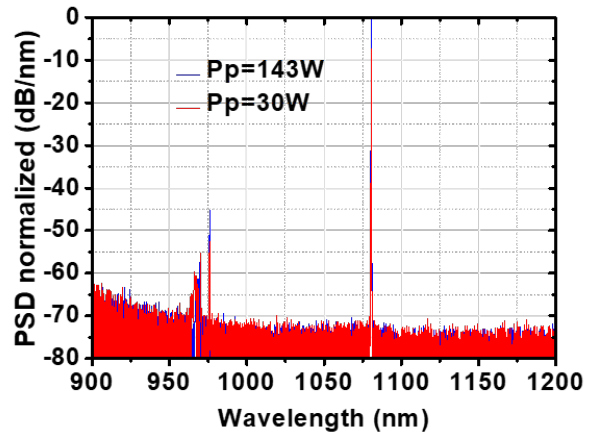


Fig. 3. Experimental spectra at the output of the seeder for an input pump power of 30 W (red curve) and 143 W (blue curve).

Fig. 4 represents the recorded temporal trace, at the oscillator's output, for an output signal power of 2 W.

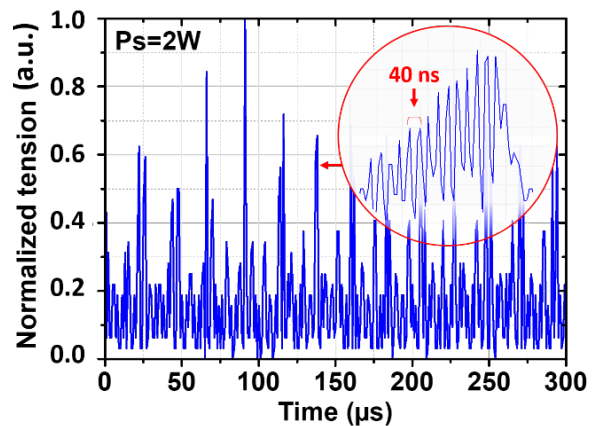


Fig. 4. Temporal signal recorded at the output of the seeder for a signal power of 2 W.

We observe, in Fig.4, that a periodic pulse train has been emitted thus meaning our oscillator is not fully locked. Also,

the signal is quite unstable seeing the power difference between the pulses. Furthermore, we observe through the inset, zooming on one of the pulses, that the intra-pulse exhibits fast oscillations with a mean period of 40 ns, corresponding to the round-trip time of light inside the cavity. In addition, we measure a mean temporal width at half maximum for the pulse envelope of 500 ns.

In Fig.5, we plot the evolution of the repetition rate of our unlocked oscillator as a function of output pump power. We observe the repetition rate evolves linearly when increasing the pump power and goes up to 170 kHz at 153 W. This temporal behavior and frequency evolution can be interpreted as signatures of passive self-Q-switching laser signals using a saturable absorber [13]. Usually, this phenomenon occurs in a cavity having a long piece of active fiber because of the reabsorption of the laser photons in the unpumped part of the fiber or occurs in heavily doped ytterbium fibers due to the quenching effect [14,15]. In our case, the physical reason for the Q-switching dynamics may not be explained in the same way since the YDF length used as the gain medium in the oscillator is very short. The underlying phenomena causing the self-Q-switched laser may be linked to the very low level of absorbed pump power in the short YDF coupled with the low reflectivity output coupler. Thus, the YDF plays the role of the gain medium as well as the saturable absorber self-modulating the losses and so creating the impulsions as in a common passively Q-switched laser [16,17]. In the literature, self-pulsing laser sources have already been used for SC generation [17,18].

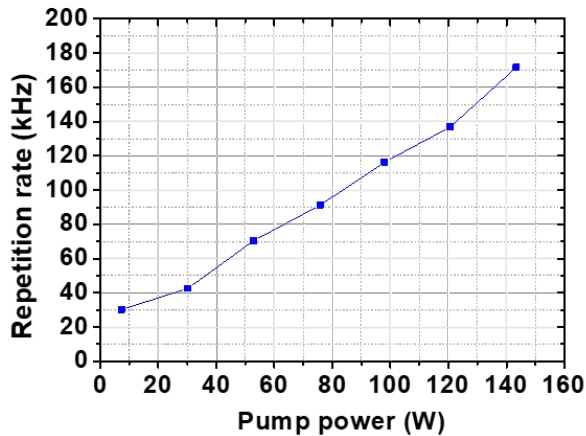


Fig.5. Evolution of the repetition rate as a function of input pump power.

### Supercontinuum generation in active double-clad large mode area

Following our oscillator, we splice an amplification stage, constituting the PSOA system. This amplification stage consists of 25 m of 20/400 DC-LMA-YDF, the same one used for the oscillator, bent over a diameter of 20 cm. We plot, in Fig. 6, the spectrum evolution at the output of

the amplifying fiber, using the pulse train emitted by the oscillator as a pump, for different signal powers. At a total output power of 90 W, we obtain a supercontinuum spectrum going from 1080 nm to 1600 nm at -30 dB of the 1135 nm peak.

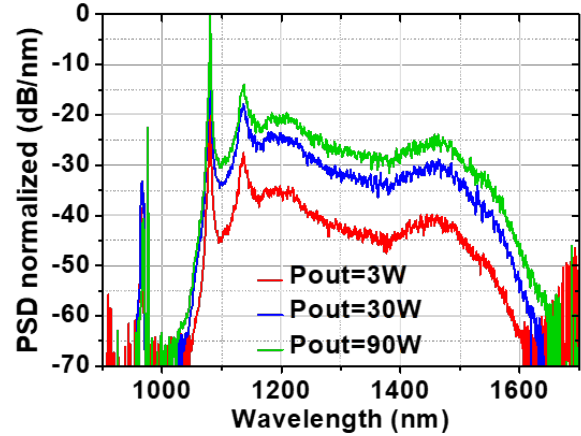


Fig. 6. Experimental SC spectra at the output of the amplifier stage for an output power going from 3 W to 90 W.

In the whole paper, we use numerical filters and integrate the area under the curve of each part of the spectra in order to split the output power between the residual pump power  $P_{p-residual}$ , the signal power at 1080 nm  $P_s$  and the power dedicated to the supercontinuum  $P_{supercontinuum}$ :

$$(1) \quad P_{out} = P_{p-residual} + P_s + P_{supercontinuum}$$

Thanks to this method, we evaluate the power dedicated to the supercontinuum of about 48 W, corresponding to 53.5 % of the total output power at the maximal pump power of 143 W.

We estimate the zero-dispersion wavelength of our amplifying fiber is around 1.3  $\mu\text{m}$  reckoning the guide dispersion could be neglected compared to the material one. Thus, initially our system evolves in the normal dispersion regime and should, in theory, broad symmetrically due to self-phase modulation [19]. However, we have to consider the absorption spectrum of the ytterbium. Indeed, every generated wavelength through nonlinear effects, shorter than the signal's, is reabsorbed by the doped fiber due to the absorption cross-section and is remitted to higher wavelengths. Furthermore, the extension of the spectrum toward the higher wavelengths is attributed to the cascaded stimulated Raman scattering [13]. Also, those spectra are quite similar to the ones obtained in the literature [20,21].

## Enhancing the supercontinuum generation in the nonlinear stage

To further increase the broadening of the supercontinuum spectrum, a 30 m-long passive germanium doped fiber is spliced to the output of the PSOA. The GDF is firstly bent over a spool with a diameter of 15.5 cm to promote the single-mode propagation into the core. However, this bending introduced spectral-dependent additional losses that had not only limited the spectral expansion but also created a strong heat load over the whole GDF. Indeed, for the 15.5 cm bending diameter, the higher wavelengths spread out from the core and are propagated into the cladding being responsible for the increase in temperature of the latter. Because of the abnormal elevation of the heat of the GDF curved at 15.5 cm, we stopped the measurement at the pump power of 112 W. To overcome this problem, we tested different bending diameters and found an optimal diameter curvature for the GDF of about 30 cm, allowing us to reduce the heat load up to 20 °C (from 53 °C to 33 °C). Thus, no cooling system was used for this section of the set-up. As shown in Fig. 7, the curvature of 30 cm helped to reach a maximum spectral broadening up to 2200 nm at -30 dB (compared to the 1135 nm peak) while the curvature of 15.5 cm restricted the spectrum up to 1650 nm at -30 dB.

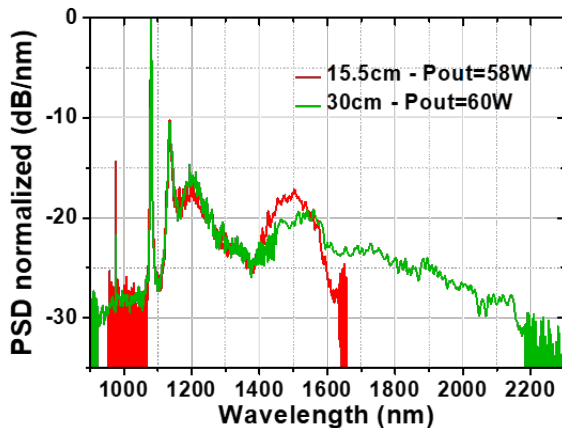


Fig.7. Evolution of the SC spectra as a function of bending diameter of 15.5 cm (red curve) and 30 cm (green curve), for a pump power of 120 W

At the output of the GDF, we measure an average output power of 82 W (with 90 W at the input) when the pump power is about 143 W. This time, using the same numerical filter as before, the SC power represents 49.6 % (40.7 W) of the output power while 49.6 % is at 1080 nm and 0.8 % at 976 nm. Furthermore, Fig. 8 highlights the differences in the SC spectrum at the output of the YDF and the GDF. We notice the spectrum is extended from [1080; 1650] nm at -30 dB to [750; 2200] nm at -30 dB of the 1135 nm peak after splicing the GDF. Indeed, this time we are not limited by the ytterbium absorption and thus supercontinuum can extend below the pump wavelength.

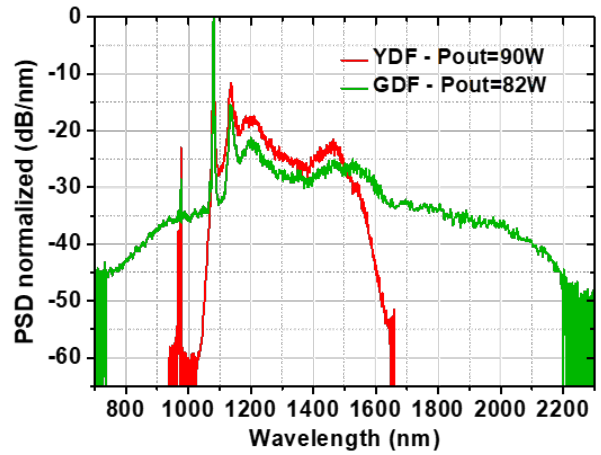


Fig.8. Spectrum evolution before (red curve) and after (green curve) the passive fiber at the pump power of 143 W.

The temporal dynamics of the GDF output is still a pulsed signal at the nanosecond range with average repetition rate values increasing as for the pump power. The evolution of the pulse repetition rate is shown in Fig. 9 with the temporal signal at pump powers of 53 W and 143 W. It is quite similar to the repetition rate out of the YDF but lower compared to the seeder repetition rate evolution for the same pump power values. As the averaged values of the repetition rate coming from the YDF are the same as the output of the GDF, the modification of the repetition rate comes directly from the YDF. It can be due to the mutual influence between the backward ASE of the amplifier stage and the oscillator stage, a higher level of ASE resulting in a lower level of population inversion that naturally shifts the repetition rate to lower values, the available gain getting smaller.

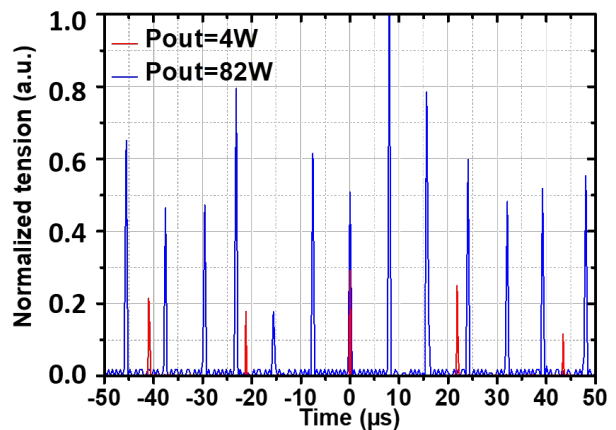


Fig.9. Temporal signal recorded at the output of the passive fiber for a signal power of 4 W (red curve) and 82 W (blue curve).

## 4. CONCLUSION

In this article, we proposed a simple method for supercontinuum generation based on an original all-fiber PSOA system simply made of a short all-fiber oscillator spliced to an active 20/400 double cladding fiber then a passive 20/400 double cladding fiber. The short cavity length of the seeder allowed us to get an 11 W self-pulsed Q-switched laser at 1080 nm. Thanks to the emission of a pulse train, we generate enough peak power in the 25 m-long active ytterbium fiber to generate a supercontinuum spectrum. At the output of our amplifying stage, our SC spectrum went from 1080 nm to 1650 nm at -30 dB with an average output power of 48 W. Then, using a long piece of passive silica fiber, we were able to increase the span of our spectrum from 750 nm to 2200 nm with an average SC power of 40.7 W.

**Acknowledgements.** The authors thank the National Association for Research and Technology (ANRT) and the company CILAS for granting the thesis of Mrs. Abbouab. We also thank the help of Vincent Couderc, Sebastien Fevrier and Yann Leventoux for the nonlinear process understanding behind the extension of the supercontinuum.

**Disclosures.** The authors declare no conflicts of interest.

**Data availability.** Data underlying the results presented in this paper are not publicly available at this time but may be obtained from the authors upon reasonable request.

## REFERENCES

- [1] T. Kääriäinen and T. Dönsberg, "Active hyperspectral imager using a tunable supercontinuum light source based on a MEMS Fabry – Perot interferometer," *Opt. Lett.*, vol. 46, no. 22, pp. 5533–5536, 2021.
- [2] M. Kumar *et al.*, "Stand-off detection of solid targets with diffuse reflection spectroscopy using a high-power mid-infrared supercontinuum source," *Appl. Opt.*, vol. 51, no. 15, pp. 2794–2807, 2012.
- [3] A. Mukherjee, S. Von Der Porten, and C. K. N. Patel, "Standoff detection of explosive substances at distances of up to 150 m," *Appl. Opt.*, vol. 49, no. 11, pp. 2072–2078, 2010.
- [4] H. H. P. T. Bekman, J. C. Van Den Heuvel, F. J. M. Van Putten, and H. M. A. Schleijsen, "Development of a Mid-Infrared Laser for Study of Infrared Countermeasures Techniques," *Technol. Opt. Countermeas.*, vol. 5615, pp. 27–38, 2004, doi: 10.1117/12.578214.
- [5] L. Jiang, R. Song, J. He, and J. Hou, "714 W all-fiber supercontinuum generation from an ytterbium-doped fiber amplifier," *Opt. Laser Technol.*, vol. 161, pp. 1–6, 2023.
- [6] T. Qi, Y. Yang, D. Li, P. Yan, M. Gong, and Q. Xiao, "Kilowatt-Level Supercontinuum Generation in Random Raman Fiber Laser Oscillator With Full-Open Cavity," *J. Light. Technol.*, vol. 40, no. 21, pp. 7159–7166, 2022.
- [7] L. Zhao *et al.*, "Generation of 215 W supercontinuum containing visible spectra from 480 nm," *Opt. Commun.*, vol. 425, pp. 118–120, 2018, doi: 10.1016/j.optcom.2018.04.066.
- [8] H. Zhang *et al.*, "Supercontinuum generation of 314.7 W ranging from 390 to 2400 nm by tapered photonic crystal fiber," *Opt. Lett.*, vol. 46, no. 6, pp. 1429–1432, 2021, doi: 10.1364/OL.420707.
- [9] H. Lin *et al.*, "10.6 kW high-brightness cascade-end-pumped monolithic fiber lasers directly pumped by laser diodes in step-index large mode area double cladding fiber," *Results Phys.*, vol. 14, p. 102479, 2019, doi: 10.1016/j.rinp.2019.102479.
- [10] L. Zeng, X. Wang, B. Yang, H. Zhang, and X. Xu, "A 3.5-kW near-single-mode oscillating – amplifying integrated fiber laser," *High Power Laser Sci. Eng.*, vol. 9, pp. 1–7, 2021, doi: 10.1017/hpl.2021.31.
- [11] Y. Zheng, Z. Han, Y. Li, F. Li, H. Wang, and R. Zhu, "3.1 kW 1050 nm narrow linewidth pumping-sharing oscillator-amplifier with an optical signal-to-noise ratio of 45.5 dB," *Opt. Express*, vol. 30, no. 8, pp. 12670–12683, 2022.
- [12] A. Hideur, T. Chartier, C. Ozkul, and F. Sanchez, "Dynamics and stabilization of a high power side-pumped Yb-doped double-clad fiber laser," *Opt. Commun.*, vol. 186, pp. 311–317, 2000.
- [13] S. V. Chernikov, Y. Zhu, J. R. Taylor, and V. P. Gapontsev, "Supercontinuum self-Q-switched ytterbium fiber laser," *Opt. Lett.*, vol. 22, no. 5, pp. 298–300, 1997.
- [14] A. V. Kir'yanov and Y. O. Barmenkov, "Self-Q-switched Ytterbium-doped all-fiber laser," *Laser Phys. Lett.*, vol. 3, no. 10, pp. 498–502, 2006, doi: 10.1002/lapl.200610039.
- [15] A. Martinez-Rios, I. Torrs-Gomez, G. Anzueto-Sanchez, and R. Selvas-Aguilar, "Self-pulsing in a double-clad ytterbium fiber laser induced by high scattering loss," *Opt. Commun.*, vol. 281, pp. 663–667, 2008, doi: 10.1016/j.optcom.2007.10.006.
- [16] M. F. A. Rahman *et al.*, "Ytterbium doped fiber saturable absorber for a stable passively Q-switched fiber laser in the 1- micron region," in *Journal of Physics: Conference Series*, 2019, pp. 1–5, doi: 10.1088/1742-6596/1151/1/012008.
- [17] D. Jin, R. Sun, S. Wei, C. Hong, J. Liu, and P. Wang, "High Pulse-energy Generation from a Monolithic Yb-doped All-fiber Dual-cavity Laser with Fiber-based Passive Q-switch," in *Advanced Solid State Lasers*, 2014, vol. AM5A.40, pp. 8–10.
- [18] S. Lin *et al.*, "Nonlinear dynamics of four-wave mixing, cascaded stimulated Raman scattering and self Q-switching in a common-cavity ytterbium/Raman random fiber laser," *Opt. Laser Technol.*, vol. 134, p. 106613, 2021, doi: 10.1016/j.optlastec.2020.106613.
- [19] T. Sylvestre *et al.*, "Recent Advances in Supercontinuum Generation in Specialty Optical Fibers," *J. Opt. Soc. Am. B*, vol. 38, pp. F90–F103, 2021.
- [20] L. Wang *et al.*, "Simple method for high average power supercontinuum generation based on Raman mode locking in a quasi-CW fiber laser oscillator," *Opt. Lett.*, vol. 47, no. 22, pp. 5809–5812, 2022.
- [21] L. Jiang *et al.*, "Kilowatt-level supercontinuum generation in a single-stage random fiber laser with a half-open cavity," *High Power Laser Sci. Eng.*, pp. 1–





